

Ho³⁺/Er³⁺ CO-DOPED Bi₂MoO₆ LUMINESCENT MATERIALS: SYNTHESIS, STRUCTURE, AND MULTICOLOR EMISSIONS

Đến tòa soạn: 21-05-2025

**Nguyen Van Hai^{1*}, Nguyen Thi Bang Bang¹, Hoang Nhu Van², Do Danh Bich¹,
Ho Van Cuu³, Nguyen Viet Long³**

¹Hanoi National University of Education, ²Phenikaa University, ³Sai Gon University

*Email: hainv@hnue.edu.vn

TÓM TẮT

VẬT LIỆU PHÁT QUANG Bi₂MoO₆ ĐỒNG PHA TẠP Ho³⁺/Er^{3+₂}: TỔNG HỢP, CẤU TRÚC, PHÁT XẠ ÁNH SÁNG ĐA MÀU SẮC

Trong bài báo này, hệ thống vật liệu phát quang đồng pha tạp Ho³⁺/Er³⁺ trên nền bismuth molybdate (Bi₂MoO₆, kí hiệu BMO) được tổng hợp thành công bằng phương pháp đốt cháy. Cấu trúc tinh thể, hình thái, thành phần nguyên tố và tính chất quang đã được khảo sát chi tiết. Kết quả nhiều xạ tia X cho thấy vật liệu BMO và BMO:Ho³⁺,Er³⁺ có cấu trúc đơn pha orthorhombic. Vật liệu BMO:Ho³⁺,Er³⁺ phát ra ánh sáng xanh lục mạnh dưới kích thích bằng bức xạ khả kiến theo cơ chế phát xạ chuyển đổi xuôi (down-conversion, DC) và phát ra ánh sáng xanh lục, vàng và đỏ khi được kích thích bằng ánh sáng hồng ngoại gần theo cơ chế phát xạ chuyển đổi ngược (up-conversion, UC). Ánh sáng của nồng độ Er³⁺ đến tính chất phát quang chuyển đổi ngược đã được xác định. Dưới kích thích bằng laser 975 nm, hai đỉnh phát xạ được ghi nhận tại 544 nm và 659 nm, tương ứng với các chuyển tiếp từ mức ⁵S₂-⁵F₄ và ⁵F₅ về mức cơ bản ⁵I₈. Các chất phát quang BMO:Ho³⁺/Er³⁺ thể hiện khả năng phát quang đa sắc mạnh chứng tỏ rằng vật liệu đã tổng hợp có tiềm năng ứng dụng lớn trong các thiết bị LED và quang điện tử.

Keywords: BMO phosphor; Ho³⁺/Er³⁺ co-doped; Photoluminescence; Light emitting diodes.

1. INTRODUCTION

Rare-earth-doped inorganic luminescent materials have gained widespread utilization in recent years across diverse applications - including general lighting, display systems, fluorescent tagging, and safety indicators - due to their superior chemical stability and environmental sustainability [1]. However, certain luminescent materials continue to exhibit limitations such as a low color rendering index (CRI), elevated correlated color temperature (CCT), reduced quantum efficiency, and inadequate thermal stability. At present, researchers are actively working to overcome these challenges through two primary strategies. The first strategy involves tuning the type and concentration of

dopant ions to enhance the CRI and lower the CCT. The second approach focuses on the development of novel host materials with superior luminescent properties to improve quantum efficiency and thermal stability [2]. Therefore, the development of high-performance phosphors with broad application potential has become a major research focus.

In luminescent materials, the host matrix plays an important role in governing their optical and luminescent properties. An ideal host material should exhibit high thermal and chemical stability, a robust and stable crystal structure, facile synthesis, cost-effectiveness, and excellent dispersion capability for rare-earth dopant ions. Recently, several high-performance molybdate-based phosphors

were reported, such as $\text{Bi}_2\text{xMoO}_6\text{:xEu}^{3+}$ [3], which emitted intense red light; $\text{Bi}_2\text{MoO}_6\text{:Yb}^{3+}/\text{Er}^{3+}/\text{Tm}^{3+}$ [4], which demonstrated excellent thermal stability; $\text{Bi}_2\text{MoO}_6\text{:Er}^{3+}/\text{Yb}^{3+}$ [5], $\text{Bi}_2\text{MoO}_6\text{:Yb}^{3+}/\text{Er}^{3+}/\text{W}^{6+}$ (20% mole: Yb^{3+} ; 2% mole: Er^{3+} , W^{6+}) [6], $\text{Bi}_2\text{MoO}_6\text{:Ho}^{3+}/\text{Yb}^{3+}$ [7], and $\text{Bi}_2\text{O}\text{-GeO}_2\text{-Na}_2\text{O}\text{-Ga}_2\text{O}_3\text{:Er}^{3+}/\text{Ho}^{3+}$ [8], all of which exhibited high luminescence efficiency; and $\text{Bi}_2\text{MoO}_6\text{:Nd}^{3+}/\text{Yb}^{3+}$ [9], which was capable of near-infrared (NIR) emission. To date, alongside the utilization of ultraviolet (UV) and visible light, increasing attention was directed towards the harvesting of NIR light. Among the various approaches, the most effective method for exploiting NIR light was doping rare-earth metal ions into semiconductor crystal lattices to take advantage of their abundant energy levels through a process known as UC luminescence. UC luminescence was a phenomenon in which NIR light was converted into visible or UV light through mechanisms such as multiphoton absorption or energy transfer [4-8]. Trivalent rare-earth ions, such as Ho^{3+} , Er^{3+} , Tm^{3+} , and Pr^{3+} , were commonly chosen as activator ions for UC luminescence due to their multiple energy levels, which facilitated radiative transitions. In particular, Ho^{3+} and Er^{3+} ions were extensively studied due to their multiple emissions in both the visible and infrared regions. However, because of their unsuitable energy levels, Ho^{3+} ions could not be efficiently excited directly at a wavelength of 975 nm [7]. In contrast, Er^{3+} ions could be efficiently excited by high-power laser diodes at 975 nm. Consequently, co-doping with $\text{Ho}^{3+}/\text{Er}^{3+}$ ions could enhance UC luminescence under NIR irradiation [8].

To the best of our knowledge, there were no prior publications on $\text{Ho}^{3+}/\text{Er}^{3+}$ co-

doped BMO host. Accordingly, in this study, $\text{Ho}^{3+}/\text{Er}^{3+}$ co-doped BMO samples with varying molar concentrations were successfully synthesized. The BMO host material, characterized by its low phonon energy, effectively facilitated efficient UC luminescence processes. Under excitation with a high-power laser diode ($\lambda_{\text{ex}} = 975$ nm), the optimal concentrations of the rare-earth ions were determined by analyzing the emission intensities in the visible region.

2. MATERIALS AND METHODS

2.1. Synthesis of $\text{Ho}^{3+}/\text{Er}^{3+}$ co-doped BMO

All chemicals used in the experiments were of analytical grade and were used without further purification. The $\text{Ho}^{3+}/\text{Er}^{3+}$ co-doped BMO materials with x% Ho^{3+} and y% Er^{3+} were synthesized by a combustion method using urea as the fuel with a molar ratio of urea to BMO of 20 : 1. The combustion technique offered several advantages, such as short reaction times and high reaction temperatures, which were achieved through exothermic combustion reactions. Initially, aqueous solutions of $\text{Bi}(\text{NO}_3)_3$, $(\text{NH}_4)_6\text{Mo}_7\text{O}_{24}$, $\text{Ho}(\text{NO}_3)_3$, and $\text{Er}(\text{NO}_3)_3$ were mixed in a molar ratio of $\text{Bi} : \text{Mo} : \text{Ho} : \text{Er} = (200 - x - y) : 100 : x : y$ to form a homogeneous solution. Urea, which served both as fuel and reducing agent, was then slowly added to the solution under magnetic stirring and heated to approximately 80 °C. After stirring and removing water vapor, a moist salt mixture was obtained. This moist mixture was transferred to a crucible, covered, and subjected to combustion at 400 °C for 4 hours. The resulting material was naturally cooled to room temperature and ground using an agate mortar. Finally, the obtained powder was annealed at 600 °C for 2 hours to ensure complete phase formation

and enhance the crystallinity of the material [10]. The synthesis conditions, including the molar ratios of the precursor salts and combustion temperature, were carefully optimized to ensure the proper incorporation of Ho^{3+} and Er^{3+} ions into the BMO matrix. The annealing step was essential to improve the crystallinity and luminescent properties of the synthesized phosphors, which were then characterized for their structural, optical and luminescent properties.

2.2. Characterization

The crystal structure of the synthesized samples was determined by powder X-ray diffraction (XRD) using a Bruker D8-Advance diffractometer. The diffraction patterns were analyzed to identify the phase purity and crystallinity of the materials. Energy-dispersive X-ray spectroscopy (EDX) was employed to determine the elemental composition of the samples, utilizing a HORIBA detector (model 7593-H) coupled with a HITACHI S-4800 field emission scanning electron microscope (FESEM). The morphological features of the synthesized samples were examined through scanning electron microscopy (SEM, HITACHI S-4800), providing insights into the surface structure and particle size distribution. UV-Vis diffuse reflectance spectra were obtained using a UV-Vis spectrophotometer (JASCO V-770), allowing for the evaluation of the optical absorption characteristics of the materials in the ultraviolet and visible regions. Photoluminescence spectra for both DC and UC emissions were recorded using a Nanolog fluorescence spectrometer (Horiba Jobin Yvon). These measurements were crucial for analyzing the luminescent properties and efficiency of the materials under different excitation conditions, providing insights into their

potential applications in lighting and display technologies.

3. RESULTS AND DISCUSSION

3.1. Structural and Morphological Analysis

To examine the structural characteristics of the materials, BMO and BZO samples doped with 2% Ho^{3+} and 7% Er^{3+} were synthesized, and their XRD patterns were obtained, as shown in Fig. 1.

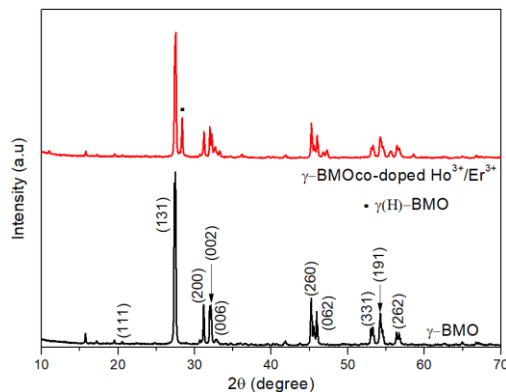


Fig. 1. XRD patterns of BMO and $\text{BMO:2\%Ho}^{3+}, 7\%\text{Er}^{3+}$.

Fig. 1 indicated that γ -BMO (koechlinite) was the predominant phase, with lattice parameters $a = 5.502 \text{ \AA}$, $b = 16.210 \text{ \AA}$, and $c = 5.483 \text{ \AA}$, consistent with JCPDS card number 21-0102 and belonging to the orthorhombic space group $Pca2_1$ [5, 7, 10]. Additionally, the diffraction peak intensities of the $\text{Ho}^{3+}/\text{Er}^{3+}$ -doped samples were lower compared to the undoped BMO, suggesting that the incorporation of trivalent rare-earth ions disrupted the cationic ordering within the crystal lattice. No secondary phases or impurities were detected in the doped samples. Nevertheless, XRD analysis revealed the presence of monoclinic modification of bismuth molybdate, $\gamma(\text{H})\text{-Bi}_2\text{MoO}_6$ (as denoted in [10]), which formed at temperatures exceeding 600°C . Subsequently, the elemental composition of the $\text{BMO:Ho}^{3+}, \text{Er}^{3+}$ material was

examined using EDX, as illustrated in Figure 2.

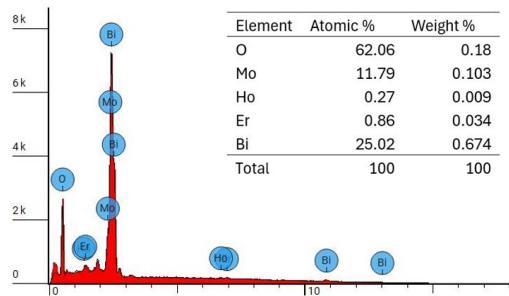


Fig. 2. EDX spectrum of BMO:2% Ho^{3+} ,7% Er^{3+} .

The results displayed in Fig. 2 confirmed the presence of Bi, Mo, O, Ho, and Er elements in the sample, with no detectable impurity signals, indicating a high level of compositional purity. The measured atomic ratios of Bi : Mo : Ho : Er = 203.6 : 96 : 2.2 : 7 closely matched the theoretical stoichiometry of 191 : 100 : 2 : 7, further validating the successful incorporation of dopant ions into the host lattice. To further explore the optical properties of the synthesized material, particularly its photon absorption behavior, UV-Vis spectroscopy was employed to determine the optical band gap energy (E_g).

The examination of UV-Vis absorption spectra show that the BMO:2% Ho^{3+} , $y\%$ Er^{3+} materials strongly absorbed radiation in the near ultraviolet and green regions. Moreover, the E_g values for the as-prepared materials were determined to be approximately 2.70 eV, corresponding to an excitation wavelength of 459 nm. This obtained E_g value was lower compared to the reported values of 2.87 - 2.97 eV [11].

The surface morphology of the material and the particle size distribution diagram in nanometer units were also determined, as shown in Fig. 3.

The results in Fig. 3 showed that the obtained material particles had a spherical-like shape, with a tendency to

distribute separately, and the average particle size was approximately 64.4 nm.

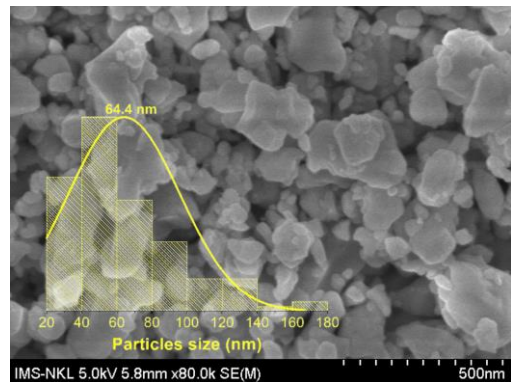


Fig. 3. SEM image of BMO:2% Ho^{3+} ,7% Er^{3+} .

3.2. Down and up-conversion properties

3.2.1. Down-conversion transitions

To find the appropriate concentration of Ho^{3+} , the fluorescence spectra of the BMO: $x\%$ Ho^{3+} sample were recorded using an excitation wavelength of 452 nm, where characteristic visible luminescence transitions of Ho^{3+} were observed: $^5\text{S}_2$ → $^5\text{F}_4$ (544 nm, blue) and $^5\text{F}_5$ → $^5\text{I}_8$ (659 nm, red) with comparable intensities. Furthermore, the best luminescence intensity reached its maximum at a concentration of 2% Ho^{3+} , so this concentration was chosen for co-doping with Er^{3+} . Next, the effect of Er^{3+} concentration on the fluorescence performance of the BMO:2% Ho^{3+} , $y\%$ Er^{3+} material was investigated (Fig. 4).

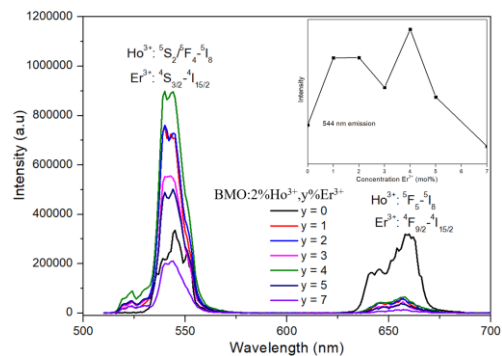


Fig. 4. The DC emission spectra of BMO:2% Ho^{3+} , $y\%$ Er^{3+} .

Fig. 4 showed that the doping of Er^{3+} into the BMO:2% Ho^{3+} material did not change the position of the absorption peaks, but the intensity showed significant changes. Specifically, the Er^{3+} doped sample increased the intensity of the blue emission ($^5\text{S}_2/{}^5\text{F}_4 \rightarrow {}^5\text{I}_8$) and decreases the intensity of the red emission (${}^5\text{F}_5 \rightarrow {}^5\text{I}_8$) compared to the undoped sample. This indicated that the Er^{3+} ion, acting as a sensitizer, enhanced the material's absorption, thereby increasing the luminescence intensity. Furthermore, when Er^{3+} was doped, the blue emission exhibited high purity, suggesting that the emission wavelength of the material could be effectively tuned towards blue light, which was suitable for applications requiring short wavelengths. Additionally, the results from Fig. 6 also showed that the blue emission intensity was strongest at an Er^{3+} concentration of 4 mol%. At higher Er^{3+} concentrations, a quenching effect occurred, leading to a decrease in the emission intensity. The optimal concentrations of 2% Ho^{3+} and 4% Er^{3+} were both higher than the optimal concentrations of 0.5% Ho_2O_3 and 0.5% Er_2O_3 reported in reference [8].

The color coordinates, color purity, and correlated color temperature of the phosphors were calculated, and the results showed that the $\text{Ho}^{3+}/\text{Er}^{3+}$ co-doped samples had high color purity, and their color coordinates fell within the blue region according to the International Commission on Illumination (CIE) system.

3.2.2. Up-conversion transitions

The UC emission spectra of the BMO:2% Ho^{3+} ,y% Er^{3+} samples were recorded under optical excitation at a wavelength of 975 nm. In the wavelength range from 500 to 700 nm, two emission bands originating from the radiative

transitions within the erbium and holmium ions were observed. Specifically, the UC emission spectra of the BMO:2% Ho^{3+} ,y% Er^{3+} system shifted significantly towards the red region. This indicated that the synthesized material had the ability to generate a rich range of colors depending on the excitation wavelength. Based on the energy levels of Ho^{3+} and Er^{3+} [4-8, 12], the process of NIR radiation excitation, energy transfer, and emission of Ho^{3+} ions was illustrated in Fig. 5.

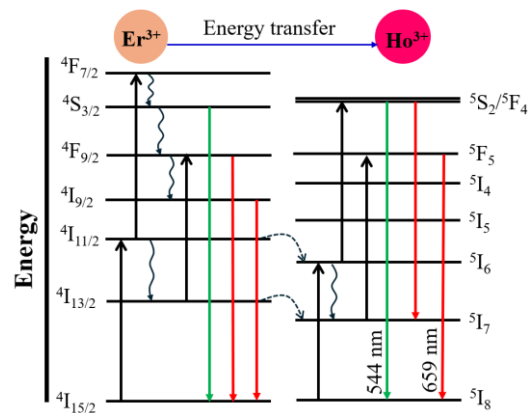


Fig. 5. Schematic illustration for the energy transfer mechanism of BMO:2% Ho^{3+} ,y% Er^{3+} .

According to Fig. 5, under 975 nm excitation wavelength, Tb^{3+} ions transition from the ground state ${}^4\text{I}_{15/2}$ to the excited state ${}^4\text{I}_{11/2}$. In this state, some Er^{3+} ions were further excited to the ${}^4\text{F}_{7/2}$ level, while other Er^{3+} ions transferred energy to the ${}^5\text{I}_6$ state of Ho^{3+} , as these two energy levels were quite close. Similarly, from the ${}^4\text{I}_{13/2}$ state, Er^{3+} ions could be excited to the ${}^4\text{F}_{7/2}$ level or transferred the energy to the ${}^5\text{I}_7$ state of Ho^{3+} . From the ${}^4\text{F}_{7/2}$ state, Er^{3+} ions relaxed to lower energy states through non-radiative transitions. After energy transfer, the ${}^5\text{I}_7$ and ${}^5\text{I}_6$ states of Ho^{3+} ions were excited to the corresponding ${}^5\text{F}_5$ and ${}^5\text{F}_4$ levels. From here, Ho^{3+} ions returned to the ground state, producing blue emission (${}^5\text{S}_2/{}^5\text{F}_4 \rightarrow {}^5\text{I}_8$) and red emission

($^5F_5 \rightarrow ^5I_8$). Additionally, the color coordinates of the samples according to the CIE were shown in Fig. 6.

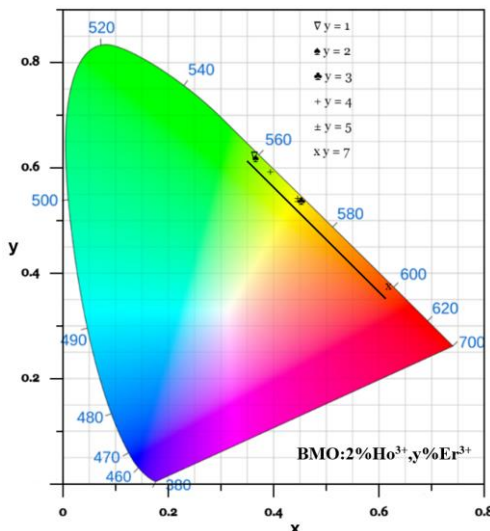


Fig. 6. CIE chromaticity diagram of $BMO:2\%Ho^{3+},y\%Er^{3+}$ under 975 nm laser diode excitation

Fig. 6 also showed that the $BMO:2\%Ho^{3+},y\%Er^{3+}$ materials exhibited clear UC emission with tunable colors ranging from blue to red, depending on the Er^{3+} content. These results indicated that the Ho^{3+}/Er^{3+} doped BMO materials were promising candidates for solid-state lighting applications and safety signage. To compare the fabrication methods in the study of BMO materials doped with rare-earth ions such as Ho^{3+} and Er^{3+} , the common chemical synthesis could be presented and compared in terms of efficiency, cost, and applications of rare-earth doped BMO or Fe oxides [13]. To further enhance the material's performance and application scope, future studies should explore for synthesis of rare-earth BMO by the polyol processes and the heat treatment processes. Thus, under NIR excitation at 975 nm, by varying the dopant concentration, the synthesized phosphors exhibited strong emissions in both the blue and red regions, indicating their potential as

phosphor materials for energy conversion devices. This feature could be particularly useful in agricultural lighting, as it enabled the simultaneous emission of blue and red light - the two primary absorption bands of chlorophyll.

4. CONCLUSION

The $BMO:Ho^{3+}$, Er^{3+} phosphors, synthesized via the combustion method, exhibit a single-phase γ -BMO (koechlinite) structure with excellent luminescent properties under both DC and UC excitation. Optimal DC performance was achieved with 2 mol% Ho^{3+} and 4 mol% Er^{3+} , producing blue-emitting phosphors with a high color purity of approximately 98% under 452 nm excitation. The gradual enhancement of red/blue emission intensity ratio with increasing Er^{3+} content under UC conditions further demonstrated its spectral tunability. These characteristics position the $BMO:Ho^{3+}$, Er^{3+} system as a strong candidate for integration into optoelectronic components, including LED lighting, optical sensors, safety signage, and photonic devices used in electronics and telecommunications.

REFERENCES

- [1]. Z. Yu, C. Zhang, X. Lou, R. Zuo, Y. Yang, G. Jia (2023). Rare earth ions doped Bi_2MoO_6 luminescent materials: Pechini sol-gel synthesis, down-conversion and up-conversion multicolor emissions, and potential applications. *Ceramics International*, **49**(15), 25987-25997
- [2]. M.J. Xu et al (2020). Structure, tunable luminescence and thermal stability in Tb^{3+} and Eu^{3+} co-doped novel $KBaIn_2(PO_4)_3$ phosphors. *Journal of Luminescence*, **221**, 117115
- [3]. I. M. Pinatti et al (2022). Tailoring Bi_2MoO_6 by Eu^{3+} incorporation for enhanced photoluminescence emissions. *Journal of Luminescence* **243**, 118675

- [4]. T. Zhenga et al (2021). Dual-center thermochromic $\text{Bi}_2\text{MoO}_6:\text{Yb}^{3+}$, Er^{3+} , Tm^{3+} phosphors for ultrasensitive luminescence thermometry. *Journal of Alloys and Compounds* **890**, 161830
- [5]. R. Adhikari et al (2014). $\text{Er}^{3+}/\text{Yb}^{3+}$ co-doped bismuth molybdate nanosheets upconversion photocatalyst with enhanced photocatalytic activity. *Journal of Solid State Chemistry* **209**, 74–81
- [6]. W. Ge, K. Liu, P. Yang, S. Deng, L. Shen (2021). Synthesis and upconversion luminescent properties of $\text{Bi}_2\text{MoO}_6:20\% \text{Yb}^{3+}, 2\% \text{Er}^{3+}$ hollow microsphere with different W^{6+} ions doping. *Journal of Solid State Chemistry* **297**, 122064
- [7]. S. Jin et al (2017). Preparation and improved photocatalytic activities of $\text{Ho}^{3+}/\text{Yb}^{3+}$ codoped Bi_2MoO_6 . *Materials Chemistry and Physics* **199**, 107e112
- [8]. T. Ragin et al (2018). Up-conversion luminescence in low phonon heavy metal oxide glass co-doped with $\text{Er}^{3+}/\text{Ho}^{3+}$ ions. *Photonics Letters of Poland*, **10** (1), 2-4
- [9]. P. V. Tumrama, P. R. Kautkara, S.P. Wankhedeb, S.V. Moharil (2019). NIR emitting $\text{Bi}_2\text{MoO}_6:\text{Nd}^{3+}/\text{Yb}^{3+}$ phosphor as a spectral converter for solar cells. *Journal of Luminescence* **206**, 39–45
- [10]. B. Senthilkumar, R. K. Selvan, L. Vasylechko, M. Minakshi (2014). Synthesis, Crystal Structure and Pseudocapacitor Electrode Properties of γ - Bi_2MoO_6 Nanoplates. *Solid State Sciences*, **35**, 18-27
- [11]. Ya.Nan Zhu et al (2026). Morphology, photocatalytic and photoelectric properties of Bi_2MoO_6 tuned by preparation method, solvent, and surfactant. *Ceramics International*, **42(15)**, 17347-17356
- [12]. H. Li et al (2018). Hydrothermal synthesis and infrared to visible up-conversion luminescence of $\text{Ho}^{3+}/\text{Yb}^{3+}$ co-doped Bi_2WO_6 nanoparticles. *Advanced Powder Technology*, **29(5)**, 1216-1221
- [13] N.V. Long, Y. Yang, T. Teranishi, C.M. Thi, Y. Cao, M. Nogami (2015). Related magnetic properties of CoFe_2O_4 cobalt ferrite particles synthesised by the polyol method with NaBH_4 and heat treatment: new micro and nanoscale structures. *RSC Advances*, **5(70)**, 56560-56569.